UNIVERSITÄT
SALZBURG

Evaluating the Impact of Iris Image Compression on Segmentation and Recognition Accuracy

Christian Rathgeb   Andreas Uhl   Peter Wild

Department of Computer Sciences

Technical Report Series

Evaluating the Impact of Iris Image Compression on Segmentation and Recognition Accuracy

Christian Rathgeb, Andreas Uhl, and Peter Wild

Abstract—A comprehensive study of the effects of lossy image compression on iris biometrics is presented. The compression standards Jpeg (JPG), Jpeg-2000 (J2K) and Jpeg-XR (JXR) are applied in numerous specified scenarios utilizing different segmentation and feature extraction algorithms in order to investigate impacts on recognition accuracy. Augmenting existing evaluations, this work examines not only the optimal choice of compression algorithms and rates, but also emphasizes segmentation issues resulting from compressed images. In addition, the impact of image compression on template protection techniques is elaborated.

Experimental results confirm, that (1) J2K outperforms JPG and JXR for compression prior to normalization, (2) the choice of where to employ compression in the iris processing chain plays an important role, as well as (3) whether one or both compared images are compressed; (4) for high compression rates, the impact on segmentation is most critical, and (5) despite the fact that template protection schemes are highly sensitive to signal degradation, compression can be successfully applied to such technologies.

Index Terms—Biometrics, iris recognition, image compression, iris segmentation, biometric template protection, Jpeg, Jpeg-2000, Jpeg-XR;

I. INTRODUCTION

IRIS RECOGNITION [1], [2] is one of the most deployed biometric applications, standardized by the International Civil Aviation Organization (ICAO) for use in future passports, and one of the technologies in the Unique Identification Authority of India (UID) project to uniquely identify people. However, the increasing market saturation of biometric instead of conventional access control methods raises the need for efficient means to store such data. The International Organization for Standardization (ISO) specifies iris biometric data to be recorded and stored in (raw) image form (ISO/IEC FDIS 19794-6), rather than in extracted templates (e.g. iris-codes). On the one hand, such deployments benefit from future improvements (e.g. in feature extraction stage) which can be easily incorporated (except sensor improvements), without re-enrollment of registered users. On the other hand, since biometric templates may depend on patent-registered algorithms, databases of raw images enable more interoperability and vendor neutrality [3]. These facts motivate detailed investigations of the effect of image compression on iris biometrics in

C. Rathgeb, A. Uhl and P. Wild are with the Multimedia Signal Processing and Security Lab (Wavelab), Department of Computer Sciences, University of Salzburg, A-5020 Salzburg, Austria (e-mail: {crathgeb,uhl,pwild}@cosy.sbg.ac.at).
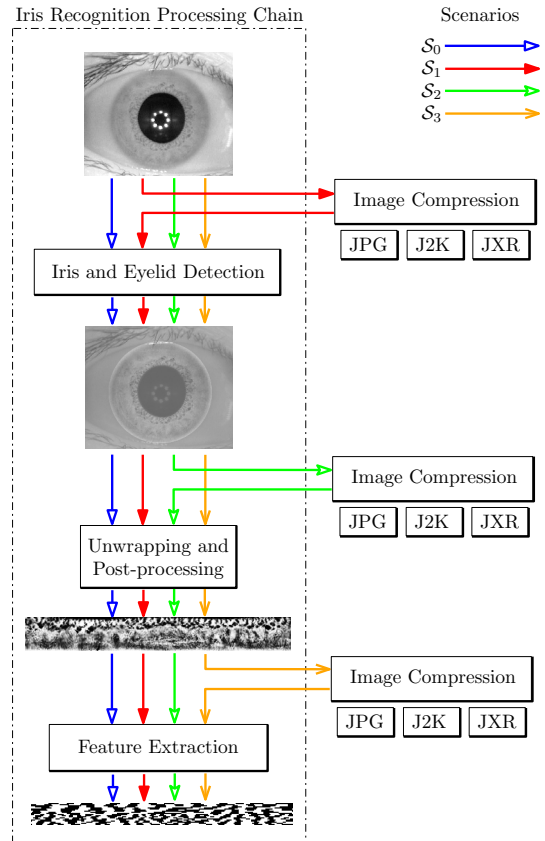
Fig. 1. Considered scenarios: No compression ($\mathcal{S}_0$), Compression of the original image after acquisition ($\mathcal{S}_1$), Compression of the ROI-encoded image after segmentation ($\mathcal{S}_2$), Compression of iris texture after normalization ($\mathcal{S}_3$).

order to provide an efficient storage and rapid transmission of biometric records. Furthermore, the application of low-powered mobile sensors for image acquisition, e.g. mobile phones, raises the need for reducing the amount of transmitted data.

Previous evaluations (e.g. [4], [11], [3]) confirm the applicability of lossy image compression in iris biometric systems, however, there is a need for more comprehensive analysis distinguishing between different application scenarios, i.e. the point in the iris processing chain, where compression is applied. As will be shown using a common data set, compression's impact on accuracy largely depends on the type of application scenario, e.g. whether templates extracted from compressed images are compared to ones generated from uncompressed or compressed images. Such discrimination has been commonly neglected in literature so far. Furthermore, it is not clear, which module of a common processing chain

TABLE I
SUMMARIZED RESULTS FOR DIVERSE STUDIES OF COMPRESSION ALGORITHM'S IMPACT ON IRIS RECOGNITION IN LITERATURE.

Ref.	Compression	Scenarios	Results	Remarks
[4]	J2K	S_3	0% EER until 0.3 bpp	4 feature extraction algorithms
[5]	JPG, J2K, SPIHT, PRVQ, FRAC	S_1	∼50% FRR at 0.01% FAR	perf. deg. if only one image is compressed
[3]	JPG, J2K	S_1, S_2	0.24% EER (vs. 0.11%) for J2K 1:150	only 4 compression rates
[6]	JPG, J2K	S_1	∼1.6% (vs. 1.45%) FRR at 0.1% FAR J2K	study of various effects (iris radius, etc.)
[7], [8]	JPG	S_1, S_3	∼4% EER (vs. ∼3%) for 1:15	study of quantization matrices
[9]	J2K	S_1	4.45% EER (vs. 1.35%) for J2K 1:100	compressed vs. uncompressed studies
[10]	JXR, J2K	S_3	∼1.9% EER (vs. ∼1.3%) for 0.4 bpp	execution speed studies

in biometric systems (acquisition, segmentation, or feature extraction) is most suitable to incorporate a distinct type of compression standard. Until now related work has focused on specific scenarios and/or algorithms only, whereas the proposed work aims at providing a more comprehensive overview.

A. Contribution of Work

The contribution of this work is a comprehensive analysis of the effects of image compression on iris biometrics. As opposed to existing investigations, image compression is applied at various positions within a common iris biometric processing chain yielding three different scenarios.

1) *Scenario S_1*: image compression is applied to the original image of the eye, i.e. no preprocessing is applied prior to image compression (e.g. in [9], [7]).
2) *Scenario S_2*: after detecting the inner and outer boundaries of the iris, non-iris regions are substituted using different gray levels, i.e. segmentation is alleviated or even lead in a certain direction (e.g. in [3]).
3) *Scenario S_3*: image compression is applied to preprocessed iris textures, i.e. normalized iris textures resulting from an unrolling process and subsequent illumination enhancement are compressed (e.g. in [4], [11]).

All three scenarios, which are illustrated in Fig. 1, are evaluated for different feature extraction algorithms in both modes, compressed vs. compressed as well as compressed vs. uncompressed. In order to clearly interpret obtained results in terms of recognition accuracy, an in-depth analysis of the issue of iris segmentation under image compression is given. Since segmentation errors typically make subsequent recognition impossible, performance is significantly degraded. In addition, the impact of image compression to a template protection scheme [12], which is considered highly sensitive to any kind of intra-class variations, is investigated to round off experimental studies.

B. Organization of Article

This article is organized as follows: Section II reviews related work regarding image compression in iris recognition. Subsequently, in Section III different compression standards and their impact on image quality are introduced. Then the effects of image compression on recognition accuracy are examined based on diverse predefined scenarios in Section IV, where emphasis is put on segmentation issues. Studies on compressed vs. uncompressed probe and gallery images are presented in Section V. The effect of image compression on iris biometric template protection is examined in Section VI. Finally, concluding remarks are given in Section VII.

II. PREVIOUS WORK

Several researchers have investigated effects of image compression on iris recognition. Table I summarizes proposed approaches according to applied compression standards, considered scenarios, and obtained results. In [4] normalized iris textures of size 512×80 pixel are compressed using J2K. Subsequently, diverse feature extraction methods are applied in order to compare pairs of compressed textures. The authors observe improvement in recognition accuracy for low compression levels. A more comprehensive study based on different compression standards, including JPG as well as J2K, which are utilized to compress original iris images, is presented in [5]. Increased accuracy was achieved when comparing pairs of iris-codes, both resulting from compressed iris textures. Focusing on original iris images the authors conclude, that iris segmentation tends to fail at high compression rates. Besides, in general original iris images exhibit greater filesize compared to preprocessed texture stripes. Similar results are obtained in [11], [9], where severe compression of original iris images causes EERs as high as 4%, compared to a compression of normalized iris textures, which does not significantly decrease accuracy [4]. In order to overcome these drawbacks a region of interest (ROI) isolation was proposed in [3], i.e. non-iris regions (eyelids and sclera) are substituted using two different gray levels. Applying J2K it is found that ROI isolation leads to a two-fold reduction in filesize while enabling an easy localization of eyelid boundaries in later stages. For a filesize of 2000 bytes only 2-3% of bits in extracted templates change, while recognition accuracy is maintained. In [13] a similar approach applying J2K ROI-coding to the iris region was proposed.

Regarding standardization of image compression in biometrics, the ISO/IEC 19794 standard on "Biometric Data Interchange Formats" represents the most relevant one. With respect to iris biometrics (ISO/IEC FDIS 19794-6), in the most recent version only J2K is included for lossy compression and recommended for standardized iris images (IREX records) by the NIST Iris Exchange program[1]. The study in [6] gives quantitative support to the revision of the ISO/IEC 19794-6 standard. By analogy, the ANSI/NIST ITL 1-2011 standard specifies iris images to be compressed with J2K.

While it is generally conceded that the JPG compression standard is not suitable at high compression rates in [7], [8] it is shown that custom designed quantization tables in JPG significantly improve recognition performance. In [10] effects of JXR compression on iris recognition are examined. JXR

[1]NIST Iris Exchange program: http://iris.nist.gov/irex/

is found to be competitive to the current standard J2K while exhibiting significantly lower computational demands.

III. IMAGE COMPRESSION IN IRIS RECOGNITION

Experimental evaluations are carried out on the CASIAv3-interval iris database[2] and the IIT Delhi Iris Database v1[3], more specifically we evaluate all left-eye images. All images are captured under (indoor) NIR illumination, details regarding the number of provided classes and the resulting amount of genuine and impostor comparison as well as image sizes are summarized in Table II. While the IITD database consists of uncompressed images a slight JPG compression is applied to the entire CASIAv3 dataset. However, it will be shown, that slight compression has no negative impact on recognition accuracy. In the following subsections the impact of different compression standards on image quality is analyzed according to various compression rates, which are defined by the ratio of resulting average filesize compared to the average filesize of uncompressed images. We therefore measure the impact on recognition accuracy in terms of false reject rate (FRR, the rate of verification transactions with truthful claims of identity being incorrectly rejected) at a certain false accept rate (FAR, the rate of verification transactions with wrongful claims of identity being incorrectly confirmed), see ISO/IEC FDIS 19795-1, illustrated in form of Receiver Operating Characteristics curves (ROCs, plotting pairs of FAR/FRR resulting from varying the operational threshold). Furthermore, we report Equal Error Rates (EERs) of the system, i.e. the system error rate, where FRR = FAR. At all authentication attempts 7 circular texture-shifts (and according bit-shifts) in each direction are performed and the minimum Hamming Distance is returned to achieve rotation-invariance.

A. Choosing Compression Standards

In the proposed study three different types of lossy image compression standards are applied:

- **Jpeg (JPG)**: the well-established (ISO/IEC 10918) DCT-based method of compressing images. Compression ratios can be varied by using more or less aggressive divisors in the quantization phase.
- **Jpeg-2000 (J2K)**: the wavelet-based image compression standard (ISO/IEC 15444), which can operate at higher compression ratios without generating the characteristic artifacts of the original DCT-based JPG standard.
- **Jpeg-XR (JXR)**: which, like Jpeg-2000, generally provides better quality than JPG but is more efficient than J2K, with respect to computational effort. In the default configuration the Photo Overlay/Overlap Transformation is only applied to high pass coefficients prior to the Photo Core Transformation (ISO/IEC 29199-2).

Iris cameras capture digital photos of the iris patterns in human eyes. Imaging does not involve lasers or flash, instead today's commercially available solutions use infrared light

[2]The Center of Biometrics and Security Research, CASIA Iris Image Database, http://www.idealtest.org

[3]The IIT Delhi Iris Database version 1.0, http://www4.comp.polyu.edu.hk/~csajaykr/IITD/Database_Iris.htm

TABLE II
DATABASES APPLIED IN EXPERIMENTAL EVALUATIONS AND ACCORDING NUMBER OF CLASSES, GENUINE AND IMPOSTOR COMPARISONS FOR LEFT EYE IMAGES AND IMAGE SIZES.

Database	Classes	Gen. Comparisons	Imp. Comparisons	Image Size
CASIAv3	249	4464	19503	320×280
IITD	224	2240	24976	320×240

(a) Eye   (b) Iris Texture
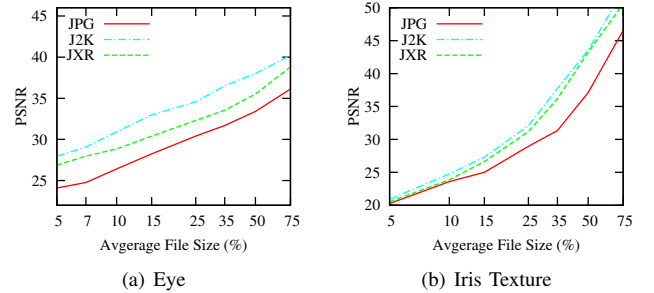
Fig. 2. Filesize vs. PSNR trade-off: quality degradation for compression of (a) original eye ($\mathcal{S}_1$), and (b) segmented texture ($\mathcal{S}_3$) images.

to illuminate the iris to be able to process also heavily pigmented iris images. Whereas specialized iris acquisition systems exist, ranging from simple handheld iris cameras, like the OKI IRISPASS-h, to completely integrated systems like the LG4000 IrisAccess system featuring two-factor and two-eye authentication, active research aims at providing sensor-independent normalization algorithms [14]. By observing compression in various different scenarios, we assess the impact on different applications taking different types of iris sensors into account.

With respect to image quality J2K and JXR reveal superior performance compared to the JPG compression standard. In Fig. 2 peak signal to noise ratio (PSNR) values are plotted for compressing original iris images and normalized iris textures (see Section IV.C) for various average filesizes. In terms of PSNR a compression of preprocessed iris textures does not affect image quality as drastic as a compression of original iris images at low compression levels. Obtained results justify the deprecation of the JPG standard in ISO/IEC FDIS 19794-6.

B. Choosing Compression Rates

In order to investigate how various scenarios affect an optimal choice of compression several different filesizes are considered for each compression standard within different scenarios. Compression rates are defined according to specific average filesize of resulting images, estimated according to the filesize of original images (which vary among scenarios), e.g. JPG-25 indicates a 1:4 filesize ratio between the JPG compressed and the corresponding reference image. Fig. 3 (a) shows a sample image of the applied database, obtained segmentation results and the extracted iris texture are shown in Fig. 3 (b)-(c).

Fig. 4 illustrates the effects of JPG-5 according to different scenarios. Obviously, a compression of preprocessed iris textures ($\mathcal{S}_3$) retains significantly more information than a compression of the original iris image ($\mathcal{S}_1$) at the same rate. For the applied dataset correctly detected "iris rings"

(a) Iris Image   (b) Segmentation

(c) Iris Texture
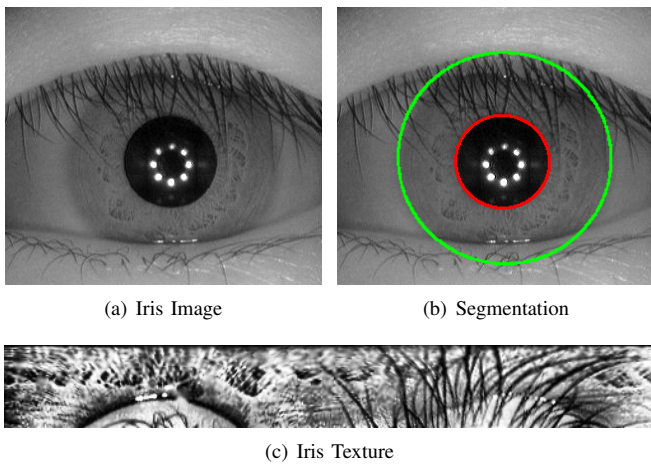
Fig. 3. Iris recognition processing chain intermediate results for uncompressed sample `S1041L01` of CASIAv3-Interval database.

(a) $\mathcal{S}_1$: Iris Image Compression   (b) $\mathcal{S}_2$: "ROI-encoded" Compression

(c) $\mathcal{S}_3$: Iris Texture Compression
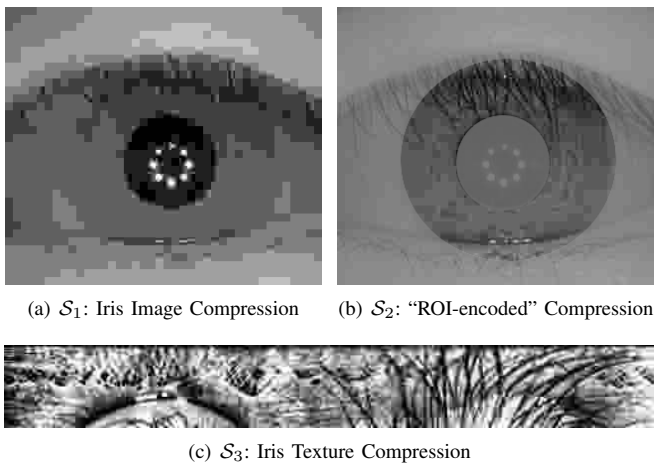
Fig. 4. JPG compression for sample `S1041L01` of CASIAv3-Interval database for various scenarios ($\mathcal{S}_1$-$\mathcal{S}_3$) obtaining relative filesize of 0.05.

(a) $\mathcal{S}_1$: Iris Image Compression   (b) $\mathcal{S}_2$: "ROI-encoded" Compression

(c) $\mathcal{S}_3$: Iris Texture Compression
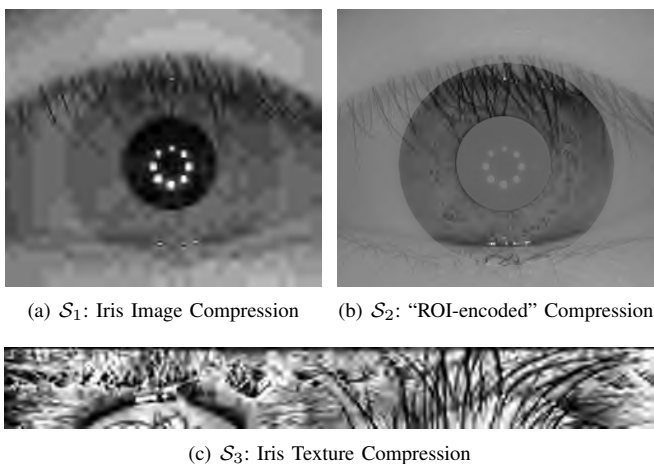
Fig. 5. J2K compression for sample `S1041L01` of CASIAv3-Interval database for various scenarios ($\mathcal{S}_1$-$\mathcal{S}_3$) obtaining relative filesize of 0.05.

(a) Ma   (b) Masek
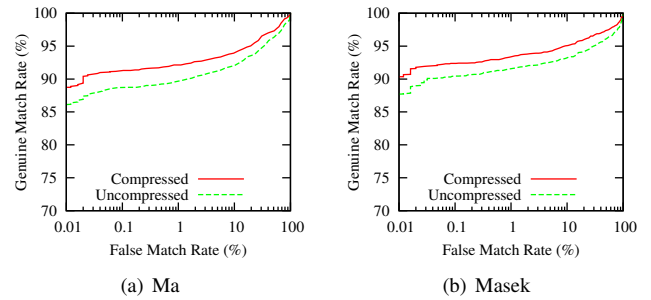
Fig. 6. Effect of slight compression on the IITD database for the feature extraction of (a) Ma and (b) Masek.

cover on average 30.86% of the entire (non-cropped) image. In case ROI-encoding is performed ($\mathcal{S}_2$), compression of non-iris regions requires negligible additional information [3], i.e. obtained image quality of the iris is equated with three-times higher compression rates of the original image (e.g. JPG-5 in $\mathcal{S}_1$ is equal to JPG-15 in $\mathcal{S}_2$). Still the scenario $\mathcal{S}_2$ appears controversial. On the one hand it is motivated by the fact that, compared to $\mathcal{S}_3$, deployed systems may benefit from future improvements in the segmentation stage. On the other hand it requires some kind of preprocessing (eyelid detection, sclera detection, etc.) which is expected to force any segmentation algorithm to detect distinct regions. In addition, the required ROI-encoding may not be available in different application scenarios, e.g. immediate transmission of image data after acquisition. Fig. 5 shows the impact of J2K compression according to different scenarios obtaining significantly improved image quality compared to the JPG compression.

IV. How Image Compression affects Accuracy

In order to provide a comprehensive analysis of the effect of image compression on recognition accuracy the impact of applied feature extraction methods as well as segmentation issues resulting from severe compression are examined with respect to the predefined scenarios.

A. Choice of Iris Database

Left-eye images of the CASIAv3 database exhibit an average filesize of 11.51kB for image sizes of 320×280 pixel. Uncompressed images (converted with lossless JPG) of the IITD databases are 15.22kB in size, on average, for smaller images of 320×240 pixel. In order to show that an initial slight JPG compression does not degrade accuracy, images of the IITD database are JPG compressed obtaining an average filesize of less than 11.51kB·240/280=9.86kB. In Fig. 6 ROC curves are plotted for uncompressed as well as compressed images of the IITD database applying different feature extractors (see Section IV. B). As observed by other authors [3], [9], a slight compression is equal to denoising, thus even slightly improved recognition rates are obtained. From an application side of view, the more challenging CASIA-v3 database, which is slightly JPEG compressed (comparable to native JPEG compression commonly implemented in iris image acquisition devices) represents a more realistic basis for experimental

evaluations than using uncompressed images as performance reference. In subsequent experiments original images of the CASIAv3 dataset are interpreted as "uncompressed" reference instances.
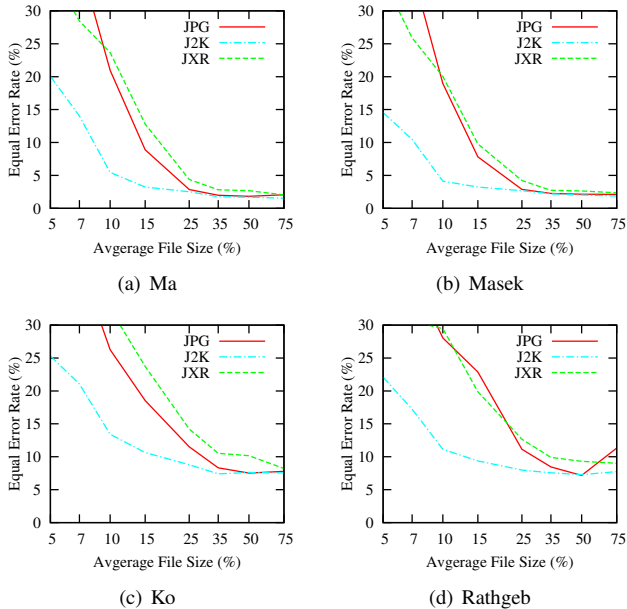
Fig. 7. Effect of compression on EERs: comparing compressed ($\mathcal{S}_1$ with $\mathcal{S}_1$) images for the feature extraction of (a) Ma, (b) Masek, (c) Ko, and (d) Rathgeb.

B. Impact on Feature Extraction Algorithms

In order to investigate the impact of image compression on recognition accuracy of diverse feature extraction methods, different custom implementations [15] of common algorithms are applied. The first one was proposed by Ma *et al.* [16]. Within this approach the texture is divided into 10 stripes to obtain 5 one-dimensional signals, each one averaged from the pixels of 5 adjacent rows, hence, the upper $512{\times}50$ pixel of preprocessed iris textures are analyzed. A dyadic wavelet transform is then performed on each of the resulting 10 signals, and two fixed subbands are selected from each transform resulting in a total number of 20 subbands. In each subband all local minima and maxima above an adequate threshold are located, and a bit-code alternating between 0 and 1 at each extreme point is extracted. Using 512 bits per signal, the final code is then $512{\times}20 = 10240$ bit. The second feature extraction method follows an implementation by Masek[4] applying filters obtained from a Log-Gabor function. Here, a row-wise convolution with a complex Log-Gabor filter is performed on the texture pixels. The phase angle of the resulting complex value for each pixel is discretized into 2 bits. To have a code comparable to the first algorithm, we use the same texture size and row-averaging into 10 signals prior to applying the one-dimensional Log-Gabor filter. The 2 bits of phase information are used to generate a binary code, which therefore is again $512{\times}20 = 10240$ bit. The

third algorithm has been proposed by Ko *et al.* [17]. Here feature extraction is performed by applying cumulative-sum-based change analysis. It is suggested to discard parts of the iris texture, from the right side [45° to 315°] and the left side [135° to 225°], since the top and bottom of the iris are often hidden by eyelashes or eyelids. Subsequently, the resulting texture is divided into basic cell regions (these cell regions are of size $8{\times}3$ pixels). For each basic cell region an average gray scale value is calculated. Then basic cell regions are grouped horizontally and vertically. It is recommended that one group should consist of five basic cell regions. Finally, cumulative sums over each group are calculated to generate an iris-code. If cumulative sums are on an upward slope or on a downward slope these are encoded with 1s and 2s, respectively, otherwise 0s are assigned to the code. In order to obtain a binary feature vector we rearrange the resulting iris-code such that the first half contains all upward slopes and the second half contains all downward slopes. With respect to the above settings the final iris-code consists of 2400 bits. Finally, we employ the iris recognition algorithm we proposed in [18]. Similar to the approach in [17] parts of the iris are discarded, [45° to 315°] and [135° to 225°]. By tracing light and dark intensity variations of grayscale values in horizontal stripes of distinct height, pixel-paths are extracted. For a height of 3 pixels each position within pixel-paths is encoded using 2 bits. For a total number of 21 stripes and a texture length of 256 pixels the resulting iris-code is of size 10752 bits.

Fig. 7 illustrates the impact of image compression on Equal Error Rates (EERs) obtained by all feature extraction algorithms. Despise the fact that some feature extraction methods require the same row-wise processing of texture stripes (which is common for iris recognition algorithms [1]) the relative effects of image compression exhibit the same characteristics (e.g. the superior accuracy of J2K compression in general and of JPG compared to JXR until an average filesize of 10%). Without loss of generality obtained results indicate an algorithm-independent effect of image compression on iris recognition.

C. Impact on Iris Segmentation

From the iris processing chain in Fig. 1 it should be clear, that compression within scenario $\mathcal{S}_1$ may affect segmentation accuracy. While for near infrared (NIR)-illuminated iris images, the outer iris-boundary typically has low contrast to the neighboring sclera regions, even for visible range iris images, segmentation may cause problems due to less pronounced pupillary boundaries. Like iris segmentation is largely affected by the database employed [14], also compression may significantly change initial image set-specific assumptions, e.g. the distribution of intensity values. We have employed two different representative segmentation algorithms to investigate the impact of compression on segmentation:

- **CAHT** [15] is a custom Hough transform-based segmentation algorithm using Canny edge detection after (database-specific) contrast adjustment to enhance pupillary and limbic boundaries. The strong assumptions about the employed dataset (CASIAv3) this algorithm was

---

[4]L. Masek: Recognition of Human Iris Patterns for Biometric Identification, Master's thesis, Univ. of Western Australia, 2003
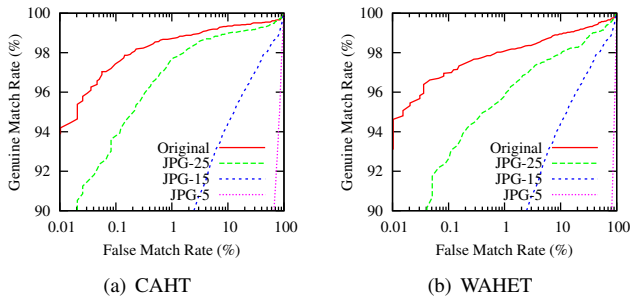
(a) CAHT   (b) WAHET

Fig. 8. Effect of image compression on different segmentation algorithms (a) CAHT (b) WAHET.

(a) Average HD   (b) False Segmentation Rate
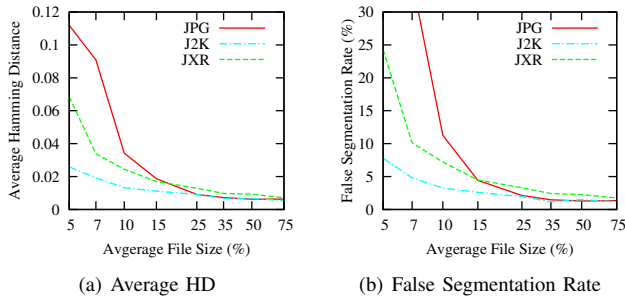
Fig. 9. Effect of image compression on segmentation masks: (a) Average HD of $\mathcal{S}_0$ vs. $\mathcal{S}_1$, and (b) rate of false segmentations per filesize.

developed for, make it a good candidate for assessing the impact on specific sensor-specific segmentation algorithms.

- **Weighted Adaptive Hough and Ellipsopolar Transforms (WAHET)** [14]: is a novel two-stage algorithm employing a weighted adaptive Hough transform iteratively refining a region of interest to find an initial center point, which is used to polar transform the image and extract polar and limbic boundary curves one after another from an (ellipso-)polar representation. This algorithm represents a more generic general-purpose segmentation algorithm, without database-specific tuning.

While the general purpose algorithm has the advantage of being more robust to changes in image recording conditions, it is generally less restrictive with respect to the pre-assumed shape (boundaries do not need to be circular). However, as can be derived visually from the compressed images in Fig. 4, especially for high compression at specific sectors there is even no clear outer boundary present any more. Therefore, holistic approaches like Hough transform turned out to be advantageous in this scenario: Fig. 8 compares the effect of compression on segmentation accuracy by estimating ROCs, i.e. measuring the total impact on recognition accuracy, for each segmentation algorithm by employing Masek's feature extraction. Nevertheless, for the remainder of comparisons we employ WAHET as segmentation algorithm, since (a) still, general-purpose algorithms are the segmentation of choice for vendor-neutral iris recognition (b) adaptive (two-stage) approaches are much faster alleviating real-time recognition and (c) even though the impact of compression on segmentation is significant, differences between segmentation algorithms are rather small.

(a) JPG   (b) J2K
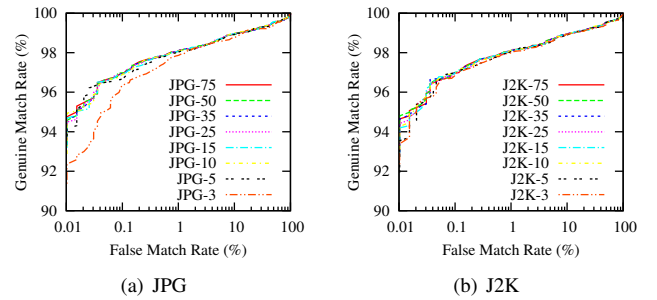
Fig. 10. Effect of iris texture compression ($\mathcal{S}_3$) on ROCs for Masek's feature extraction algorithm using (a) JPG, and (b) J2K with different filesizes.

To measure the direct impact on segmentation, we employ an $m \times n$ sized segmentation mask M for each $m \times n$ input image I:

$$M(x,y) := \begin{cases} 1 & \text{if } (x,y) \text{ iris pixel wrt. } I \\ 0 & \text{otherwise.} \end{cases} \tag{1}$$

This mask is used to estimate the average Hamming distance between the segmentation result (masks) of the compressed input versus the segmentation masks of the uncompressed, original images. For J2K only up to 2% of pixels are incorrectly classified. This amount increases drastically for JPG and JXR with resulting filesizes of 25% and above until 11% for JPG and 7% for JXR for resulting filesizes of 5%, see Fig. 9 (a). When considering a segmentation of being tolerable if its falsely classified pixels do not exceed 5% percent, we get a plot of average filesize versus false segmentation rate for each algorithm, illustrated in Fig. 9 (b). With respect to recognition performance a direct comparison of scenario $\mathcal{S}_1$ and $\mathcal{S}_2$ (see Table III) reveals the impact of segmentation errors on the overall accuracy at distinct filesizes.

D. Avoiding Segmentation Errors

For low-power sensors or continuous sensing, e.g. by remote cameras, scenario $\mathcal{S}_1$ is probably the only practicable solution, i.e. after image acquisition the full eye image needs to be compressed to reduce the amount of submitted data. But there are better solutions in case the remote sensing device offers computation resources to employ segmentation remotely, in order to avoid large impact on segmentation.

Scenario $\mathcal{S}_3$ avoids segmentation errors by employing compression after normalization. Results depicted in form of ROC curves, plotted in Fig. 10 for different resulting filesizes for the standards JPG and J2K, illustrate that in this scenario compression has much less impact on recognition accuracy. For JPG and J2K, recognition rates stay rather low at approximately 1.77-1.84 % EER, only very high compression, e.g. JPG-3, show a slightly worse recognition rate for high security applications with requested low FAR.

Another alternative to compression before segmentation is scenario $\mathcal{S}_2$ employing some sort of ROI compression after segmentation, i.e. in our experiments segmentation is conducted on the original input and the segmentation result is used to compress only parts of the input image which correspond to the iris texture. This way, segmentation is

(a) JPG   (b) J2K
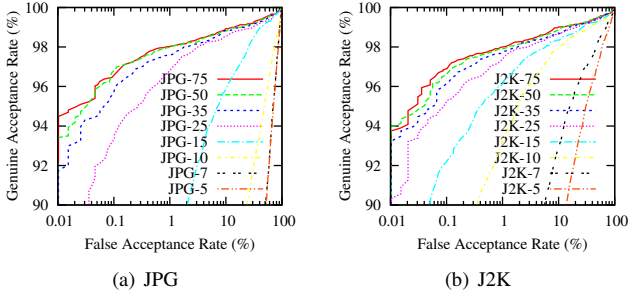
Fig. 11. Effect of ROI compression ($\mathcal{S}_2$) on ROCs for Masek's feature extraction algorithm using (a) JPG, and (b) J2K with different filesizes.

artificially simplified, but compression artifacts are yet to be mapped into Daugman's doubly dimensionless coordinate system. From the results illustrated in Fig. 11 one can see that, in contrast to scenario $\mathcal{S}_3$, this type has much more impact on recognition accuracy. However, it has to be taken into account, that compression rates refer to the original image size in $\mathcal{S}_2$, whereas the normalized iris textures compressed in $\mathcal{S}_3$ are typically much smaller in size. When considering an average iris image containing 30.86% of iris texture pixels, filesizes of 5% in $\mathcal{S}_2$ corresponds to approximately 15% in scenario $\mathcal{S}_3$ when ignoring the size impact of the artificial uniform eyelid, sclera and pupil segmentation areas illustrated in Fig. 1.

V. GALLERY VS. PROBE COMPRESSION

Since authentication attempts involve an execution of the processing chain for both, probe and gallery images, scenarios $\mathcal{S}_0 - \mathcal{S}_3$ may be applied at enrollment (for the gallery image) and/or at authentication (for the probe image). Considering the reported effect of JPG to even increase recognition accuracy as long as no severe compression artifacts occur [5] it is interesting to see, whether the compression of both images results in better or worse performance than comparing compressed with uncompressed samples, given the potential high impact on segmentation errors. Tested combinations of scenarios reflect the following applications:

- **Low-power sensor**: the sensor is capable of acquiring input images only, but does not have the ability to conduct iris segmentation. The compressed image is transferred to some computing device, which may have access to the full-sized original gallery image or feature vector extracted from this image ($\mathcal{S}_0\mathcal{S}_1$), or compressed gallery images and templates extracted from these images, respectively ($\mathcal{S}_1\mathcal{S}_1$).

- **Intelligent sensor**: within this application scenario, the sensor is specifically designed to the application domain of iris image acquisition (e.g. specialized iris cameras) and is capable of iris preprocessing, but comparison is still centralized for security issues. Still, in order to minimize the amount of transmitted information and encryption efforts, iris images should be compressed (encryption is executed after compression). This application is reflected with scenario combination $\mathcal{S}_0\mathcal{S}_2$ in case the gallery is composed of templates extracted from original uncompressed images and $\mathcal{S}_2\mathcal{S}_2$, if the same sensor is employed for enrollment.

(a) $\mathcal{S}_0\mathcal{S}_2$-JPG   (b) $\mathcal{S}_0\mathcal{S}_2$-J2K

(c) $\mathcal{S}_0\mathcal{S}_1$-JPG   (d) $\mathcal{S}_0\mathcal{S}_1$-J2K

(e) $\mathcal{S}_1\mathcal{S}_1$-JPG   (f) $\mathcal{S}_1\mathcal{S}_1$-J2K
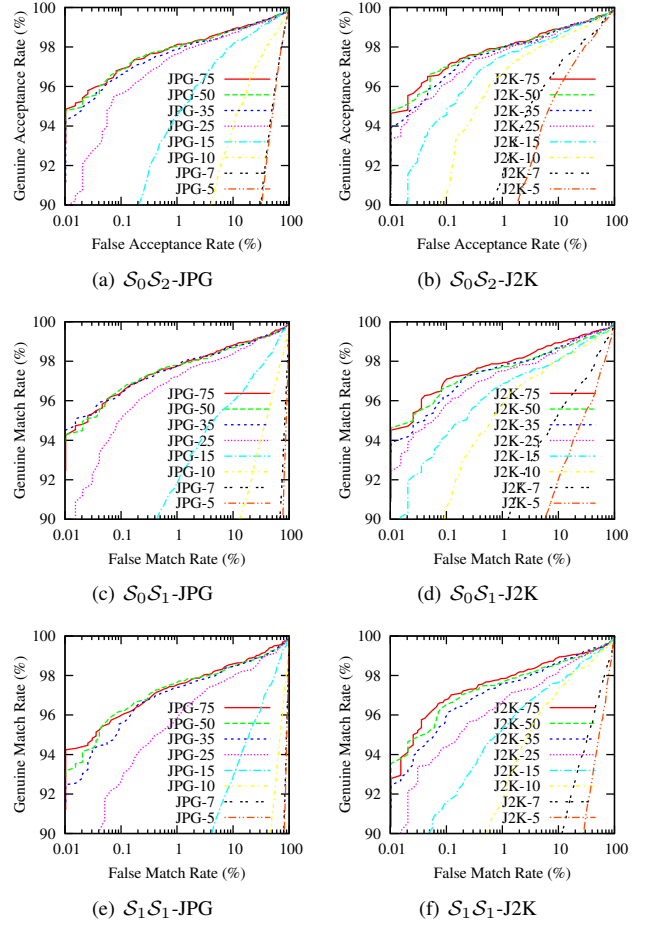
Fig. 12. Gallery vs. probe compression's effect on ROCs: (a)-(b) uncompressed vs. compressed ROI, (c)-(d) uncompressed vs. compressed originals, (e)-(f) compressed vs. compressed originals.

- **Integrated sensor**: this scenario reflects typical smartcard solutions, where both the user template and acquired probe image do not leave the integrated system and are compared on-card. Since typically resources are strictly limited on such devices, it is desirable to store relevant information only, e.g. the normalized compressed iris texture. Considering this application we are interested in, whether an additional compression of the probe image ($\mathcal{S}_3\mathcal{S}_3$) increases or decreases recognition accuracy, compared to scenario combination $\mathcal{S}_0\mathcal{S}_3$.

Table III lists the obtained EERs for the above listed combinations of scenarios for various average filesizes. Furthermore, ROC curves comparing resulting filesizes for the most prominent application scenarios $\mathcal{S}_0\mathcal{S}_1, \mathcal{S}_0\mathcal{S}_2$ and $\mathcal{S}_1\mathcal{S}_1$ are plotted for each compression standard in Fig. 12.

Regarding the low-power sensor application, one can see, that for each employed compression standard (JPG, J2K and JXR), superior performance is obtained by employing gallery templates from uncompressed instead of compressed images. For both JPG and J2K, EERs are on average 1.31 times higher in the compressed vs. uncompressed scenario, and 1.52 times higher for JXR. Interestingly, the improvement for J2K almost increases with compression rate and is very pronounced for filesizes <10%, whereas for JPG and JXR the improvement

TABLE III
EERs FOR VARIOUS SCENARIOS USING DIFFERENT COMPRESSION STANDARDS AND FILESIZES.

File Size (%)	$\mathcal{S}_0\mathcal{S}_1$			$\mathcal{S}_0\mathcal{S}_2$			$\mathcal{S}_0\mathcal{S}_3$			$\mathcal{S}_1\mathcal{S}_1$			$\mathcal{S}_2\mathcal{S}_2$			$\mathcal{S}_3\mathcal{S}_3$		
	JPG	J2K	JXR	JPG	J2K	JXR	JPG	J2K	JXR	JPG	J2K	JXR	JPG	J2K	JXR	JPG	J2K	JXR
75	1.93	1.86	2.17	1.78	1.76	1.81	1.77	1.76	1.77	2.13	1.87	2.37	1.84	1.75	1.88	1.77	1.77	1.77
50	1.98	2.09	2.33	1.79	1.88	1.95	1.77	1.76	1.76	2.14	2.02	2.65	1.80	1.87	2.15	1.77	1.77	1.76
35	1.90	2.04	2.24	1.83	1.81	2.05	1.77	1.79	1.78	2.26	2.21	2.74	1.99	1.96	2.62	1.77	1.79	1.79
25	2.23	2.17	2.60	2.00	1.88	2.37	1.77	1.78	1.81	2.88	2.69	4.23	2.30	2.07	3.95	1.77	1.81	1.80
15	4.86	2.59	5.02	3.38	2.14	4.26	1.77	1.76	1.80	7.82	3.24	9.79	5.70	2.57	8.81	1.73	1.80	1.81
10	10.94	2.92	10.00	7.30	2.42	7.90	1.81	1.78	1.78	18.96	4.14	20.04	14.21	3.59	17.44	1.79	1.78	1.83
7	28.55	5.82	14.67	16.73	4.35	11.29	-	-	-	36.08	10.47	25.89	22.20	8.05	22.27	-	-	-
5	30.95	8.57	24.85	17.11	5.67	17.31	1.79	1.77	1.86	37.66	14.56	34.82	22.55	11.29	27.99	1.83	1.74	1.90
3	-	-	-	-	-	-	1.80	1.81	1.84	-	-	-	-	-	-	1.81	1.84	1.94

is most pronounced for medium filesizes (10%, 15%).

The intelligent sensor application reveals a similar result: again compressed versus uncompressed comparison yielded better recognition accuracy for almost every compression algorithm over the entire range of tested rates (solely J2K for very low compression turned out to exhibit no perceivable difference). On average, EERs are 1.3 times higher for JPG, 1.34 times higher for J2K and 1.62 times higher for JXR, with again most pronounced improvement for medium filesizes for JXR and JPG, whereas J2K exhibits the highest improvement for filesizes <10%.

Finally, in case of the integrated sensor application it is evident, that compression has very little impact in general. EERs are in the range of 1.76-1.86% for all algorithms in scenario $\mathcal{S}_0\mathcal{S}_3$ and in the range of $1.76 - 1.94\%$ for $\mathcal{S}_3\mathcal{S}_3$. Considering these recognition results, it is advisable to stick to the fastest available implementations in this scenario and neglect the impact on recognition accuracy.

Finally, comparing the overall recognition rates, we notice that (1) J2K delivers throughout better performance than JPG, followed by JXR, (2) compressed versus uncompressed comparison ($\mathcal{S}_0\mathcal{S}_1,\mathcal{S}_0\mathcal{S}_2$) delivers better results than the corresponding compressed versus compressed application ($\mathcal{S}_1\mathcal{S}_1,\mathcal{S}_2\mathcal{S}_2$) , and (3) recognition accuracy is better in scenarios, where compression is applied late in the processing chain ($\mathcal{S}_3$ is better than $\mathcal{S}_2$, followed by $\mathcal{S}_1$).

VI. IMAGE COMPRESSION AND TEMPLATE PROTECTION

Biometric template protection schemes, which are commonly categorized as biometric cryptosystems and cancelable biometrics [19], target privacy and security risks caused by unprotected storage of biometric data (ISO/IEC FCD 24745). Meeting properties of irreversibility and unlinkability template protection systems can be applied to secure existing records within biometric databases, i.e. without re-enrollment of registered subjects. While template protection schemes are generally conceded highly sensitive to any sort of signal degradation, investigations on the impact of image compression on recognition accuracy have remained elusive.

A. Iris Biometric Template Protection

In past years several types of iris biometric template protection schemes have been proposed. First attempts to iris biometric template protection were presented in [20], where the biometric template itself (or a hash value of it) serves as
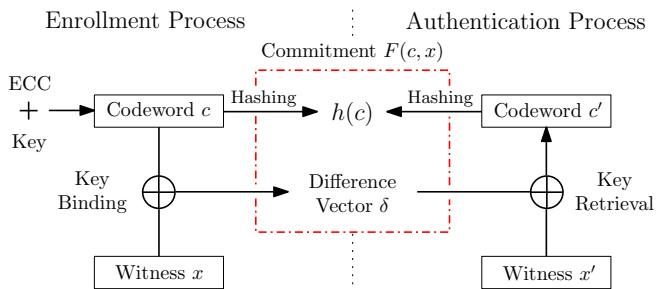
Fig. 13. Basic operation mode of the fuzzy commitment scheme.

a cryptographic key and intra-class variance is overcome by means of majority decoding. Experimental results are omitted and it is commonly expected that the proposed system reveals poor performance due to the fact that the authors restrict to the assumption that only 10% of bits of an iris-code change among different iris images of a single data subject. In general, average intra-class distances of iris-codes lie within 25-35%. Juels and Wattenberg [12] proposed the fuzzy commitment scheme (FCS), a bit commitment scheme resilient to noise. A FCS is formally defined as a function F, applied to commit a codeword $c \in C$ with a witness $x \in \{0,1\}^n$ where C is a set of error correcting codewords of length n. The witness x represents a binary biometric feature vector which can be uniquely expressed in terms of the codeword c along with an offset $\delta \in \{0,1\}^n$, where $\delta = x - c$. Given a biometric feature vector x expressed in this way, c is concealed applying a conventional hash function (e.g. SHA-3), while leaving δ as it is. The stored helper data is defined as,

$$F(c,x) = \big(h(x), x - c\big). \qquad (2)$$

In order to achieve resilience to small corruptions in x, any x' sufficiently "close" to x according to an appropriate metric (e.g. Hamming distance), should be able to reconstruct c using the difference vector δ to translate x' in the direction of x. In case $\|x - x'\| \leq t$, where t is a defined threshold lower bounded by the according error correction capacity, x' yields a successful decommitment of $F(c,x)$ for any c. Otherwise, $h(c) \neq h(c')$ for the decoded codeword c' and a failure message is returned. In Fig. 13 the basic operation mode of the FCS is shown.

The FCS was applied to iris-codes in [21]. In the scheme 2048-bit iris-codes are applied to bind and retrieve 140-bit cryptographic keys prepared with Hadamard and Reed-Solomon error correction codes. Hadamard codes are applied
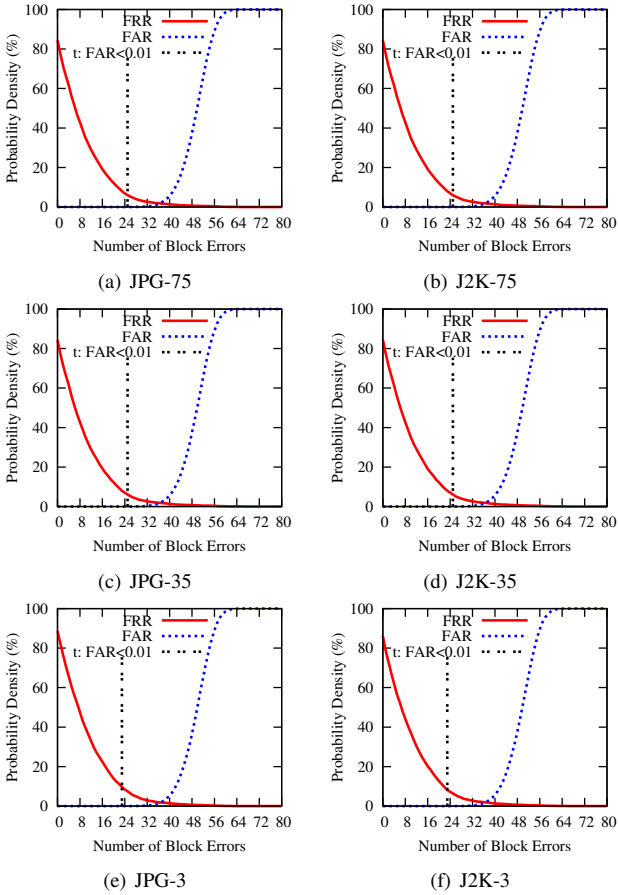
Fig. 14. Effect of compression on template protection: FRR and FAR for the proposed FCS for the Masek feature extraction algorithm using JPG and J2K for filesizes (a)-(b) 75%, (c)-(d) 35%, and (e)-(f) 3%.

TABLE IV
SUMMARIZED EXPERIMENTS APPLYING THE FEATURE EXTRACTOR OF MASEK TO FCSs FOR VARIOUS COMPRESSION STANDARDS.

File Size (%)	$\mathcal{S}_0\mathcal{S}_3$-JPG FRR at FAR≤0.01	Corr. Blocks	$\mathcal{S}_0\mathcal{S}_3$-J2K FRR at FAR≤0.01	Corr. Blocks	$\mathcal{S}_0\mathcal{S}_3$-JXR FRR at FAR≤0.01	Corr. Blocks
75	6.05	25	5.96	25	5.98	25
50	6.03	25	6.12	25	6.09	25
35	6.12	25	6.09	25	6.21	25
25	6.16	25	6.07	25	6.05	25
15	6.03	25	6.09	25	7.72	24
10	7.07	24	7.10	24	7.31	24
5	7.43	23	7.30	24	7.72	24
3	7.51	23	8.11	23	9.57	23

TABLE V
SUMMARIZED EXPERIMENTS APPLYING THE FEATURE EXTRACTOR OF MA *et al.* TO FCSs FOR VARIOUS COMPRESSION STANDARDS.

File Size (%)	$\mathcal{S}_0\mathcal{S}_3$-JPG FRR at FAR≤0.01	Corr. Blocks	$\mathcal{S}_0\mathcal{S}_3$-J2K FRR at FAR≤0.01	Corr. Blocks	$\mathcal{S}_0\mathcal{S}_3$-JXR FRR at FAR≤0.01	Corr. Blocks
75	5.04	32	5.12	32	5.32	32
50	5.04	32	5.32	32	5.37	32
35	5.12	32	5.12	32	5.37	32
25	5.07	32	5.32	32	5.49	32
15	5.45	32	5.35	32	5.88	32
10	6.14	32	5.89	32	6.35	32
5	7.22	32	6.25	32	7.45	32
3	7.34	32	6.97	32	7.89	32

to eliminate bit errors originating from the natural biometric variance and Reed-Solomon codes are applied to correct burst errors resulting from distortions. In order to provide an error correction decoding in an iris-based FCS, which gets close to a theoretical bound, two-dimensional iterative min-sum decoding is introduced in [22]. A matrix formed by two different binary Reed-Muller codes enables a more efficient decoding. Different techniques to improve the accuracy of iris-based FCSs have been proposed in [23], [24].

B. Template Protection Compression Scenario

According to previous experiments, a custom implementation of the FCS presented in [21] is evaluated applying scenario combination $\mathcal{S}_0\mathcal{S}_3$ where recognition accuracy is hardly affected by image compression. For the applied algorithm of Masek we found that the application of Hadamard codewords of 128-bit and a Reed-Solomon code $RS(16,80)$ reveals the best experimental results for the binding of 128-bit cryptographic keys. At key-binding, a $16\cdot 8 = 128$ bit cryptographic key R is first prepared with a $RS(16,80)$ Reed-Solomon code. The Reed-Solomon error correction code operates on block level and is capable of correcting $(80-16)/2 = 32$ block errors. Then the 80 8-bit blocks are Hadamard encoded. In a Hadamard code, codewords of length n are mapped to codewords of length 2^{n-1} in which up to 25% of bit errors can be corrected. Hence, 80 8-bit codewords are mapped to

80 128-bit codewords resulting in a 10240-bit bitstream which is bound with the iris-code by XORing both. Additionally, a hash of the original key $h(R)$ is stored as second part of the commitment. At authentication key retrieval is performed by XORing an extracted iris-code with the first part of the commitment. The resulting bitstream is decoded applying Hadamard decoding and Reed-Solomon decoding afterwards. The resulting key R' is then hashed and if $h(R') = h(R)$ the correct key R is released. Otherwise an error message is returned. For the algorithm of Masek and Ma *et al.* the proposed fuzzy commitment schemes yield FRRs of 5.45% and %, respectively, at a FAR of 0.01%.

Experimental results for the applied compression standards and according filesizes are summarized in Table IV and Table V, including the number of corrected block errors after Hadamard decoding (i.e. error correction capacities may not handle the optimal amount of occurring errors within intra-class key retrievals). The FRR of a FCS defines the percentage of incorrect keys returned to genuine subjects. By analogy, the FAR defines the percentage of correct keys retrieved by non-genuine subjects. Selected performance rates for FCSs under various forms of image compression are plotted in Fig. 14 (a)-(f). Focusing on the feature extraction of Masek and Ma *et al.*, the proposed FCSs provide FRRs of 5.53% and 4.25% at a FAR less than 0.01% correcting up to 25 and 32 block errors, respectively. FRRs are lower bounded by error correction capacities, i.e. bit-level error correction is applied more effectively if errors are distributed rather uniformly [25].

For all of the applied image compression standards a continuous significant degradation of recognition accuracy with respect to applied compression is observed (see Table IV and Table V). For the algorithm of Masek at the highest com-

pression FRRs of 7.51%, 8.11%, and 9.57% are obtained at FARs less than 0.01% for the JPG, J2K, and JXR compression standard. Slightly better results are obtained for the algorithm of Ma *et al.* (see Table V). While FCSs suffer from degradation in key retrieval rates under severe compression, performance improves for average compression (which is equivalent to denoising). In general, lossy image compression has little impact on main characteristics of FCSs (see Fig. 14), i.e. all types of investigated FCSs appear rather robust to a certain extent of image compression. As previously shown, J2K and JXR compression standards provide higher image quality at certain filesize with respect to PSNRs. However, higher quality according to PSNR values does not coincide with obtained recognition rates nor with key retrieval rates achieved by the applied FCSs, especially at higher compression levels.

VII. SUMMARY AND CONCLUSION

Augmenting investigations on the operability of iris recognition systems in the past, e.g. in [4], [3], [9], the proposed work pointed out various aspects and issues regarding image compression in iris biometrics. Three scenarios have been considered: (1) image compression of the original image, (2) "ROI-encoded" compression, and (3) iris texture compression after normalization. Whereas compression is most effective in the first scenario in terms of data rate reduction it has the most severe impact on recognition accuracy among tested scenarios. Detailed analysis of the impact of compression on iris recognition accuracy in this scenario revealed that a loss of recognition accuracy is caused mostly by segmentation errors. In contrast, for the remaining scenarios compression impact is found to be much lower, since segmentation is performed prior to compression. We found that comparing compressed with uncompressed images delivers superior results compared to matching compressed images only. The observed behaviour was found to be independent of the choice of feature extraction or segmentation algorithms. Throughout all experiments J2K was confirmed to deliver the best results. Surprisingly, in most cases the recent JXR standard lead to even inferior results as compared to JPG. Despite all the negative effects of severe lossy compression, denoising properties of low compression rates improve recognition accuracy throughout experiments. Regarding iris-biometric template protection all compression standards induced a slight impact on key retrieval for high compression rates, while results remained stable for low and medium compression. Again, this behavior can be explained by the fact that segmentation is performed prior to compression in the considered template protection scheme. Opposed to existing works we identify image segmentation the most critical issue when it comes to iris image compression.

ACKNOLEDGEMENT

REFERENCES

[1] K. W. Bowyer, K. Hollingsworth, and P. J. Flynn, "Image understanding for iris biometrics: A survey," *Comp. Vis. Image Underst.*, vol. 110, no. 2, pp. 281 – 307, 2008.

[2] J. Daugman, "How iris recognition works," *IEEE Trans. Circ. and Syst. for Video Techn.*, vol. 14, no. 1, pp. 21–30, 2004.

[3] J. Daugman and C. Downing, "Effect of severe image compression on iris recognition performance," *IEEE Trans. Inf. Forensics and Sec.*, vol. 3, pp. 52–61, 2008.

[4] S. Rakshit and D. M. Monro, "An evaluation of image sampling and compression for human iris recognition," *IEEE Trans. Inf. Forensics and Sec.*, vol. 2, pp. 605–612, 2007.

[5] S. Matschitsch, M. Tschinder, and A. Uhl, "Comparison of compression algorithms' impact on iris recognition accuracy," in *Proc. of the 2nd Int'l Conf. on Biometrics (ICB 2007)*, LNCS, 4642, pp. 232–241, 2007.

[6] P. Grother, "Quantitative standardization of iris image formats," in *Proc. of the Biometrics and Electronic Signatures (BIOSIG 2009)*, Lecture Notes in Informatics, pp. 143–154, 2009.

[7] M. Konrad, H. Stögner, and A. Uhl, "Custom design of jpeg quantization tables for compressing iris polar images to improve recognition accuracy," in *Proc. of the 3rd Int'l Conf. on Biometrics (ICB 2009)*, LNCS, 5558, pp. 1091–1101, 2009.

[8] G. Kostmajer, H. Stögner, and A. Uh, "Custom jpeg quantization for improved iris recognition accuracy," in *Proc. of the 24th IFIP Int'l Information Security Conf. 2009 (IFIP SEC'09)*, pp. 78–86, 2009.

[9] R. W. Ives, D. A. Bishop, Y. Du, and C. Belcher, "Iris recognition: The consequences of image compression," *EURASIP J. on Advances in Signal Processing*, vol. 2010, p. 9 pages, 2010.

[10] K. Horvath, H. Stögner, and A. Uhl, "Effects of jpeg xr compression settings on iris recognition systems," in *Proc. of the 14th Int'l Conf. on Comp. Anal. of Images and Patt.*, LNCS, 6855, pp. 73–80, 2011.

[11] R. W. Ives, R. P. Broussard, L. R. Kennell, and D. L. Soldan, "Effects of image compression on iris recognition system performance," *J. of Electronic Imaging*, vol. 17, 2008.

[12] A. Juels and M. Wattenberg, "A fuzzy commitment scheme," *Sixth ACM Conf. on Comp. and Comm. Sec.*, pp. 28–36, 1999.

[13] J. Hämmerle-Uhl, C. Prähauser, T. Starzacher, and A. Uhl, "Improving compressed iris recognition accuracy using jpeg2000 roi coding," in *Proc. of the 3rd Int'l Conf. on Biometrics 2009 (ICB'09)*, vol. 5558 of *LNCS*, pp. 1102–1111, 2009.

[14] A. Uhl and P. Wild, "Weighted adaptive hough and ellipsopolar transforms for real-time iris segmentation," in *Proc. of the 5th IAPR/IEEE Int'l Conf. on Biometrics (ICB'12)*, pp. 1–8, 2012.

[15] J. Hämmerle-Uhl, E. Pschernig, , and A.Uhl, "Cancelable iris biometrics using block re-mapping and image warping," *In Proc. of the Information Security Conf. 2009 (ISC'09) LNCS: 5735*, pp. 135–142, 2009.

[16] L. Ma, T. Tan, Y. Wang, and D. Zhang, "Efficient iris recognition by characterizing key local variations," *IEEE Trans. Image Proc.*, vol. 13, no. 6, pp. 739–750, 2004.

[17] J.-G. Ko, Y.-H. Gil, J.-H. Yoo, and K.-I. Chung, "A novel and efficient feature extraction method for iris recognition," *ETRI Journal*, vol. 29, no. 3, pp. 399 – 401, 2007.

[18] C. Rathgeb and A. Uhl, "Secure iris recognition based on local intensity variations," in *Proc. of the Int.Conf. on Image Analysis and Recognition (ICIAR'10)*, vol. 6112 of *Springer LNCS*, pp. 266–275, 2010.

[19] C. Rathgeb and A. Uhl, "A survey on biometric cryptosystems and cancelable biometrics," *EURASIP J. on Inf. Sec.*, vol. 2011, 2011.

[20] G. Davida, Y. Frankel, and B. Matt, "On enabling secure applications through off-line biometric identification," *Proc. of IEEE, Symp. on Sec. and Privacy*, pp. 148–157, 1998.

[21] F. Hao, R. Anderson, and J. Daugman, "Combining Cryptography with Biometrics Effectively," *IEEE Trans. on Computers*, vol. 55, no. 9, pp. 1081–1088, 2006.

[22] J. Bringer, H. Chabanne, G. Cohen, B. Kindarji, and G. Zémor, "Theoretical and practical boundaries of binary secure sketches," *IEEE Trans. on Inf. Forensics and Sec.*, vol. 3, pp. 673–683, 2008.

[23] C. Rathgeb and A. Uhl, "Adaptive fuzzy commitment scheme based on iris-code error analysis," in *Proc. of the 2nd European Workshop on Visual Information Processing (EUVIP'10)*, pp. 41–44, 2010.

[24] L. Zhang, Z. Sun, T. Tan, and S. Hu, "Robust biometric key extraction based on iris cryptosystem," *In Proc. of the 3rd Int'l Conf. on Biometrics 2009 (ICB'09) LNCS: 5558*, pp. 1060–1070, 2009.

[25] C. Rathgeb, A. Uhl, and P. Wild, "Reliability-balanced feature level fusion for fuzzy commitment scheme," in *Proc. of the Int'l Joint Conf. on Biometrics (IJCB'11)*, pp. 1–7, 2011.